Effect of Casein Concentration in Suspensions and Gels on Poly(ethylene glycol)s NMR Self-Diffusion Measurements

Roxane Colsenet,[†] Olle Soderman,[‡] and François Mariette*,[†]

Process Engineering Technology Research Unit, Cemagref, CS 64426, 17 avenue de Cucillé, 35044 Rennes, Cedex, France, and Physical Chemistry 1, Chemical Center, University of Lund, P.O. Box 124, S-22100 Lund, Sweden

Received June 20, 2005; Revised Manuscript Received August 16, 2005

ABSTRACT: PFG-NMR spectroscopy was used to study the diffusion of molecular probes (poly(ethylene glycol)s) in casein suspensions and gels in terms of the effects of probe molecular size (molecular mass between 1080 and 634 000 g/mol), casein concentrations (from 3.24 to 16.22 g/100 g), and effects of rennet coagulation. A strong dependency of diffusion on probe size was observed, both in casein suspensions and in gels: as the PEG size increased, the diffusion was reduced. This effect was more pronounced for higher casein concentrations. Changes in casein structure after addition of rennet increased the diffusion coefficient for 82 250 and 634 000 g/mol PEG. The PEG self-diffusion coefficients in casein gels were compared to the casein gel structures characterized by scanning electron microscopy. Assuming high internal micelle porosity, a diffusion model with two diffusion pathways, one outside and one inside the micelles, was used to explain the PEG diffusion in casein solutions and gels. The results were discussed in the context of variations in casein micelle voluminosity after renneting.

Introduction

Molecular transport, as characterized by diffusion coefficients, is a key feature of food processes, particularly dairy processes. For example, the transformation of milk into cheese involves many operations, such as coagulation, draining, salting, and ripening, in which water and solute diffusion are important parameters affecting the microbiological and sensorial stability of cheeses. Caseins represent 80% of protein content and are directly involved in the formation of dairy gels. Providing a quantitative description of solute diffusion in casein gels should therefore contribute significantly to the rationalization of dairy processes.

The pulsed field gradient NMR (PFG-NMR) technique is a powerful tool that can be used to measure polymer self-diffusion coefficients in suspensions and gels, and measurements can be performed on a wide range of different polymers. It is noninvasive and yields self-diffusion coefficients of high accuracy in reasonable measuring times. In addition, because of recent hardware development, it is now possible to measure very low diffusion coefficients (values down to $\sim 10^{-15}$ m^2 s^{-1} have been measured[1]).

Poly(ethylene glycol)s (PEGs) were selected as probes, offering a series of key advantages: a broad range of molecular weights can be covered, and a polydispersity factor close to one which prevents complications arising from molecular weight distribution effects is achievable. Moreover, weak interactions with proteins[2−6] make it possible to observe the obstruction effects induced by proteins in various porous structures. The obstruction effects relate to the increase in path length for diffusion caused by the slowly moving protein molecules.

Some studies have already reported on PEG self-diffusion (D) in different systems (in solution,[7−16] in gel state,[7,11,12,17−22] in cartilage,[23] and in wet cotton[24]) measured by pulsed field gradient NMR or other techniques (release kinetics data[17] and use of radioactive markers[7]). The results show a strong dependency of PEG diffusion on concentrations and on the structure of the matrix. Independently of the investigated system, the PEG diffusion decreases with increasing matrix polymer concentrations. In addition, for the same PEG molecular mass, the diffusion will be affected by the polymer structure, and there is a difference in the reduction in D/D_0 for similar matrix concentrations with D_0 the PEG self-diffusion coefficient in pure water.

Johansson et al.[7] measured PEG diffusion (1118 g/mol) in κ-carrageenan gels at two KCl concentrations: at 10 mM D/D_0 was 0.73 and at 100 mM D/D_0 was 0.83 for a carrageenan concentration of 6 g/100 g. They explained this difference by the structure modifications of the gel induced by KCl. At 100 mM, KCl induced aggregation of the carrageenan chains into rather thick fibers with a diameter of around 50 Å, whereas significantly thinner fibers were observed at 10 mM KCl. Thicker fibers result in larger spaces between the fibers and thus to a less hindered pathway for diffusing molecules of finite size. Dextran diffusion has already shown a modification induced by KCl.[25] The authors concluded that the polymer self-diffusion was a convenient method to obtain information on the solution/gel transition.

In curdlan gels,[22] D/D_0 for 1000 g/mol PEG was 0.65 at a matrix concentration of 6 g/100 g. Compared to the diffusion data of Johansson et al.,[7] the PEG diffusion was slower, showing that diffusion of PEG depends on the details of the obstruction generated by the matrix. Other studies have shown a size dependency on PEG diffusion in polymer solutions,[8−11] polymer gels,[11,22] cartilage,[23] and wet cotton.[24] The main finding in these studies was a decrease in PEG diffusion when the PEG size increased for the same network. For example, in a poly(vinyl alcohol) (PVA) system[9] at a given concentration of 20 g/100 g, D/D_0 was 0.41 for 200 g/mol PEG, 0.27 for 1000 g/mol PEG, and 0.21 for 4000 g/mol PEG.

[†] Cemagref.
[‡] University of Lund.
* Corresponding author: Tel 33 (0)223482121; fax 33(0)-223482115; e-mail Francois.Mariette@cemagref.fr.

10.1021/ma051294h CCC: $30.25
Published on Web 10/04/2005

While many studies have been performed with polymer solutions and gels, only a few have focused on the gelation effect on PEG diffusion. Johansson et al.[7,26] studied the diffusion of monodisperse fractions of PEG in polymer gels and solutions of κ-carrageenan and poly(styrenesulfonate) and found an influence of the probe size, matrix concentration, and thickness and stiffness of the polymer chains constituting the network, i.e., the structure in the gels.

Masaro et al.[10] measured the self-diffusion coefficients of various PEG in solutions and gels of PVA. The PVA concentrations varied from 0 to 38 g/100 g, ranging from dilute solutions to polymer gels. In all cases, PEG diffusion decreased when the PVA concentration increased, thus during the transition from a solution to a gel, but the gelation effects overlapped with the matrix concentration effects.

Griffiths et al.[15] studied PEG self-diffusion in D_2O as a function of different PEG architectures (cyclic or linear) but for the same molecular weight. The behavior of the two architectures was found to be very different (at 5.1 g/100 g for cyclic 10 000 g/mol PEG, D/D_0 was 0.51, and at the same concentration for linear 10 000 g/mol PEG, D/D_0 was 0.41). The authors related these differences to the friction opposing the motion of the cyclic polymer being greater than that opposing the motion of the linear polymer.

The effects of variation in diffusion time Δ have not been studied by all authors. Some authors have made their self-diffusion coefficient measurements at a constant diffusion time Δ,[8−10,14,15,18,19,22,27] and possible restriction and the possibility of non-Gaussian diffusion on account of the presence of barriers were not investigated. The effects of variation in diffusion time Δ have been studied in paclitaxel aqueous solution,[13] and the PEG self-diffusion coefficient was found to be constant up to $\Delta = 350$ ms. The PEG self-diffusion coefficient decreased when Δ increased in (poly(methacrylic acid) hydrogels,[21] in stearyl taconamide/*N*,*N*-dimethylacrylamide copolymer gels,[28] in wet cotton,[24] and in cartilage.[23] Walderhaug et al.[12] investigated the diffusion time effects in the ethyl (hydroxyethyl)cellulose−sodium dodecyl sulfate system in both solutions and gels. The PEG diffusion was found to be independent of Δ in solutions, but a decrease in PEG diffusion was observed in gels at high polymer concentrations and for the largest PEG. They discussed the decrease in terms of the hierarchically intricate structures of the studied systems.

The aims of the present study were to investigate the self-diffusion coefficient of molecular probes in casein suspensions and gels, in particular with regard to the effects of probe molecular size and casein concentration. Self-diffusion coefficients were related to scanning electron microscopy images in order to understand the effects of the gel matrix structure on PEG diffusion. This work is an extension of a previous work.[29]

Materials and Methods

Materials. Native phosphocaseinate powder (INRA, Rennes, France) was used, and the powder composition is summarized in Table 1. After rehydration, 70% of the hydrated powder particles has a diameter between 200 and 315 nm.

The PEG polymers $H[(OCH_2CH_2)]_n$ OH (where n is the number of repeating units) were obtained from Polymer Laboratories (Marseille, France), with different average molecular weights ($M_w = 1080$, 8500, 82 250 and 634 000 g/mol) and low polydispersity indices ($M_w/M_n = 1.01$, 1.02, 1.02, and 1.07, respectively, as indicated by the suppliers). All polymers were used without further purification. The D_2O (purity above 99.8%) used for mixing the samples was purchased from Dr. Glaser (Basel, Switzerland). Sodium azide, NaN_3 (Merck, Darmstadt, Germany), and NaCl were used without purification. The rennet for the gel formation, with a chymosin concentration of 55 mg/L, was purchased from Pourprix (Aix-En-Provence, France).

Table 1. Composition of Micellar Casein Powder

	micellar casein powder (%)
total solids	100
total nitrogen matter	89.3
noncasein nitrogen	4.1
nonprotein nitrogen	0.5
calcium	2.9
ash	8.1
pure proteins	85.2

Sample Preparation. Rehydration of the casein powder was performed at room temperature with D_2O/NaCl solution (0.1 M). The use of D_2O reduces the interference between the proton peaks of water and PEG and improves the accuracy of the PEG peak intensity values. Sodium azide was added (0.02% w/w) to each solution to prevent bacteria development.

For convenience, PEG was added to casein suspensions (0.1% w/w) for each average molecular weight. The percentage of PEG in water was thus different for each sample and varied between 0.103% w/w for the least concentrated and 0.116% w/w for the most concentrated casein suspensions. PEG diffusion measurements in pure D_2O indicated no variation in PEG diffusion for PEG concentrations between 0.1 and 1% w/w. Consequently, small variations in PEG concentration in the casein samples have no influence on PEG self-diffusion values. The pH was measured to 6.9 in all samples.

Caseins gels were prepared from the casein suspensions by addition of rennet to a final concentration of 100 μL/10 mL. After addition of the rennet the samples were shaken vigorously, and small amounts were transferred to 5 mm NMR tubes (~1 mL). The remainder was kept in a beaker. All the samples were kept in a water bath for 2 h at 30 °C and then cooled to 20 °C. Water evaporation was checked by weighing NMR tubes before and after gelation. No significant loss of water content of the gel was observed. NMR measurements were performed after the equilibrium period of the gel (~18 h), at least 2 days after preparation of the samples. After longer periods, gel shrinkage would have occurred.

Determination of Dry Matter. The dry matter of all casein suspensions was determined by measuring variations in weight after drying in an oven for 24 h at 100 °C. Protein concentrations were calculated from values of dry matter in each casein suspension and pure protein percentage in dry matter (85.20% for caseins). The casein suspension concentrations ranged between 3.24 and 16.44 g/100 g. For the casein gel concentrations, dilution of the casein suspensions was taken into account after the addition of rennet.

NMR Self-Diffusion Measurements. The majority of the measurements were performed on a 200 MHz Bruker spectrometer, and some complementary measurements were performed on a 400 MHz Bruker spectrometer, both equipped with a field gradient probe.

Pulsed-gradient spin-echo (PGSE: 90°−τ−180°−τ−echo) and pulsed-gradient stimulated-echo (PGSTE: 90°−τ_1-90°−τ_2−90°−τ_1−echo) sequences were used to measure the PEG self-diffusion coefficient.

The diffusion coefficients were obtained using

$$\frac{I(\delta,\Delta,g)}{I_0} = \exp[-kD] \qquad (1)$$

with $k = \gamma^2 g^2 \delta^2 (\Delta - \{\delta\}/\{3\})$, and $I(\delta,\Delta,g)$ and I_0 are the echo intensities in the presence of pulse gradients of strength g and absence of pulse gradients, respectively. The length of the gradient pulse is δ, Δ is the diffusion time (corresponding to the distance between the leading edges of gradient pulses), γ

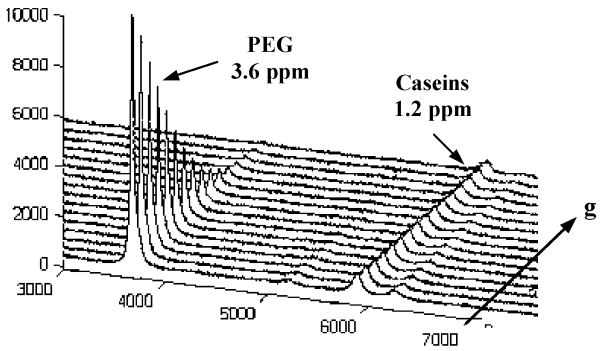

Figure 1. Spin-echo ^{1}H NMR spectra of a casein suspension 13 g/100 g containing PEG with $M_w = 634\,000$ g/mol at varying gradient intensities (g from 0.7 to 5.95 T/m) at 20 °C. The abscissa is given as channel number in the 8K spectrum. The intensities are given in arbitrary units.

is the gyromagnetic ratio (for protons, $\gamma = 26.7520 \times 10^7$ rad T^{-1} s^{-1}), and D is the self-diffusion coefficient.

In agreement with this equation, a semilogarithmic plot of echo intensities vs k is known as a Stejskal−Tanner plot.

The stimulated-echo sequence (PGSTE) was used for systems containing spins with short transverse relaxation time T_2 and long longitudinal relaxation time T_1 and to detect restriction to translational diffusion occurring during the diffusion time Δ. In a homogeneous system, the measured diffusion coefficient is independent of Δ.

NMR tubes (5 mm) were used and all the measurements were conducted at 20 ± 0.1 °C. The gradient strength g used in this study ranged between 1.07 and 9.63 T/m.

In an ordinary NMR proton spectrum, the PEG signal overlaps with casein signals at a shift of ~3.6 ppm. However, because of the very short transverse relaxation times (T_2) of casein protons compared to that of PEG protons, casein protons are severely attenuated compared to the PEG signal in the Hahn echo spectra. Therefore, in most of the measurements in this study, casein signals were negligible and did not contribute to the echo intensity.

For the PGSTE sequence the interval between the first and the second 90° pulses was increased to 30 ms to attenuate the protein signals, and the interval between the second and the third 90° pulses was adjusted to have Δ values between 40 and 400 ms.

An example of ^{1}H spectra obtained for a diffusion measurement of 634 000 g/mol PEG in casein suspension (13 g/100 g) with the PGSTE sequence is presented in Figure 1. The protein signal intensity is clearly negligible.

A total of 16 or 32 scans were collected with PGSE and PGSTE sequences with a recycle delay of 1 s. Δ was adjusted to have the same diffusion pathway for each PEG, in accordance with the Einstein equation $z = (2D_{PEG}\,\Delta)^{1/2}$ with $z \sim 2\,\mu$m. In this case the distance covered by the PEG was greater than the casein micelle diameter (diameter between 200 and 315 nm).

All the data processing was performed with Matlab or Tablecurve software. Monte Carlo simulations were used for error calculations with 100 iterations, in agreement with procedures described in ref 30.

Scanning Electron Microscopy (SEM). Small cubes of the gels (5 × 5 × 5 mm) were cut out and immersed in 2.5% v/v glutaraldehyde at room temperature for 48 h and then rinsed thoroughly three times for 10 min with distilled water, after which they were immersed in 0.2% v/v OsO_4 overnight at room temperature. The samples were rinsed several times with distilled water before being dehydrated in a graded ethanol series (10−30−50−70−80−90−95−100% (v/v)) in 20 min steps. Samples were then critical-point dried through CO_2 in a critical-point drier (CPD 010, Balzers Union Ltd., Liechtenstein). Dried samples were fractured, mounted onto specimen stubs, gold-coated, and analyzed microscopically using a scanning electron microscope (JEOL JSM 6301F) operated at an acceleration voltage of 9 kV. The images were produced by CMEBA (France, Rennes).

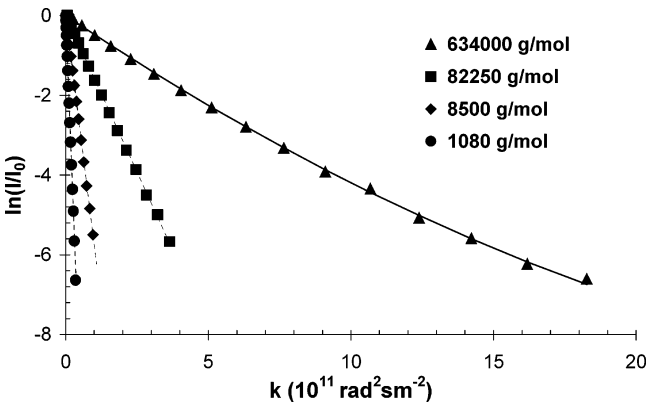

Figure 2. Stejskal−Tanner plot of PEG in water for different PEG molecular weights at 20 °C measured with the PGSE sequence. The dotted lines are linear regressions of the data, and the solid line is a fit of eq 2 with $M_w/M_n = 1.07$.

Table 2. PEG Hydrodynamic Radius Calculated with the Stokes−Einstein Equation (Eq 3) from PEG Diffusion in D_2O at 20 °C

M_w (g/mol)	M_w/M_n	D_0 (m^2 s^{-1})	R_h (nm)
1080	1.01	1.82×10^{-10}	1.18
8500	1.02	5.82×10^{-11}	3.68
82250	1.02	1.60×10^{-11}	13.39
634000	1.07	5.45×10^{-12}	39.30

Results

PEG Self-Diffusion in Pure Water. Figure 2 shows the echo attenuation of PEG diffusion in a 0.1 M NaCl solution in D_2O at 20 °C for each PEG molecular mass. The Stejskal−Tanner plots of the echo intensities were linear, except for 634 000 g/mol PEG where polydispersity effects were observed as a slight curvature in the plot.

To account for possible polydispersity effects of the polymer sample, the attenuation data were analyzed by using the method of cumulants.[31,32] In terms of a second-order cumulant expansion, the attenuation of the echo signal can be expressed as

$$\ln\left(\frac{I}{I_0}\right) = -k\langle D\rangle + \frac{1}{2}k^2\langle D\rangle^2[1 - (M_w/M_n)^{-4/5}] \quad (2)$$

where $\langle D\rangle$ is the average diffusion coefficient.

The fitting of the echo attenuation decay was performed with Tablecurve software by including the polydispersity index $M_w/M_n = 1.07$ given by the manufacturer in eq 2. The result of this treatment is shown in Figure 2 by the solid line. This result checked and confirmed that the curvature was not due to other causes that PEG polydispersity. Polydispersity was taken into account in the data processing of the 634 000 g/mol PEG results by using the method of cumulants.

The PEG hydrodynamic radius was calculated with the Stokes−Einstein equation:

$$R_h^{PEG} = \frac{kT}{6\pi\eta D_{PEG}} \quad (3)$$

T being the temperature in kelvin (293.5 K), k the Boltzmann constant (1.38×10^{-23} J K^{-1}), and η the viscosity of heavy water (1.002×10^{-3} Pa·s at 20 °C).

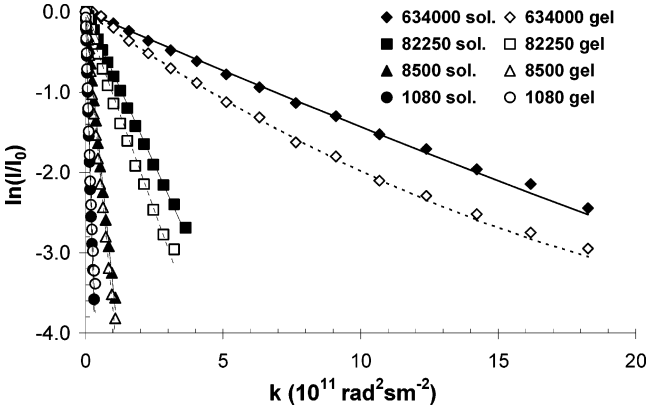

Figure 3. Stejskal−Tanner plots of PEG for different PEG molecular weights (1080, 8500, 82 250, and 634 000 g/mol) in casein suspensions (full symbols) and gels (open symbols) (16.44 g/100 g of water) at 20 °C. All the curves are linear regression, except for the PEG 634 000 g/mol in gel, which is a fit using eq 2.

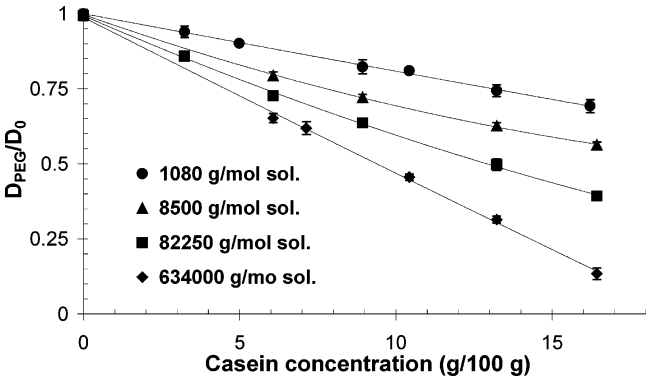

Figure 4. Plot of the normalized PEG self-diffusion coefficient in casein suspensions vs casein concentrations for different PEG molecular mass. Dashed lines are only guides for the eyes.

All these findings are summarized in Table 2 and are in accordance with other studies.[7,10] Compared to the casein radius (~125 nm), all the PEG sizes are smaller.

Determination of D_0. The self-diffusion coefficient value of PEG in D_2O/NaCl solution (0.1 M) cannot be directly used to normalize PEG self-diffusion coefficients measured in protein suspensions and gels. Indeed, there are soluble residues in protein powders such as minerals, ash, lactose, and noncasein nitrogen which contribute to PEG diffusion hindrance in the aqueous phase after rehydration. To consider only the effects of casein, we must normalize the PEG self-diffusion coefficient in casein suspensions by using the PEG self-diffusion coefficient in the water phase, including these soluble compounds[33] as D_0. Determination of this diffusion coefficient is described below.

The protein gels at two casein concentrations (9 and 18.6 g/100 g of water) were prepared with all the PEGs and centrifuged in order to extract the aqueous phase from these gels. The PEG self-diffusion coefficients and the dry matter of these aqueous phases were measured. Then linear regression was performed between dry matter and self-diffusion coefficient for each PEG in the aqueous phase. When the amounts of lactose, ash, minerals, and noncasein nitrogen are known, the percentage of soluble compounds available to be extracted from the gel can be calculated. Therefore, the self-diffusion coefficient in the soluble phase (D_0) for each PEG was predicted for each casein concentration. These

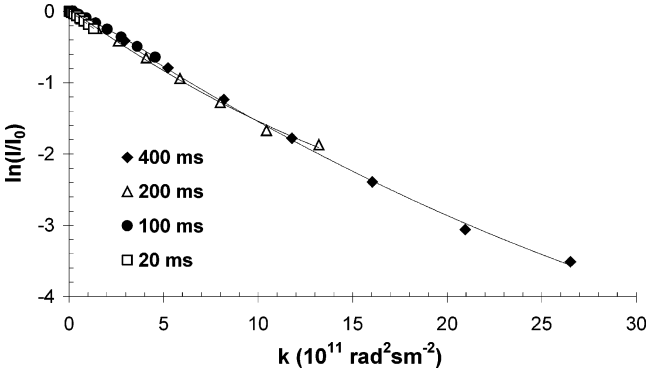

Figure 5. Stejskal−Tanner plots of PEG 634000 g/mol in casein gel (16.44 g/100 g of water) for different diffusion times Δ at 20 °C measured with a 200 MHz spectrometer and the PGSE sequence.

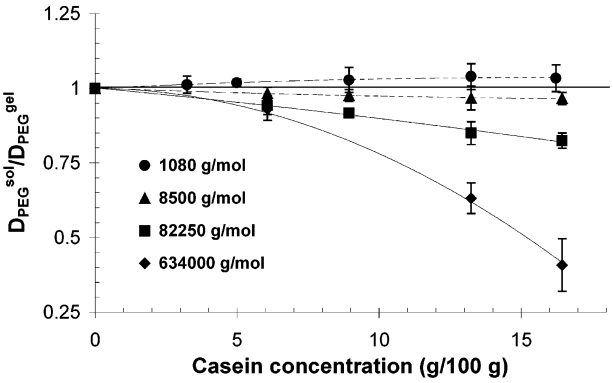

Figure 6. PEG self-diffusion coefficient in casein suspensions divided by PEG self-diffusion coefficient in casein gels vs the casein concentration for different PEG molecular masses at 20 °C. Dashed lines are only guides for easier reading.

values were used to normalize self-diffusion coefficients in casein suspensions and gels (D_{PEG}) and subsequently the reduced diffusion coefficient, defined as $D_r = D_{PEG}/D_0$.

PEG Self-Diffusion Coefficients in Casein Suspensions. The self-diffusion coefficients of all the PEGs in casein suspensions at concentrations between 3.24 and 16.44 g/100 g of water were measured at 20 °C. Examples of Stejskal−Tanner plots are given for all the PEGs in casein suspensions (16.44 g/100 g) (Figure 3). All the PEG signals decrease when the gradient strength is increased, but the signal intensity of larger PEGs decreases much less rapidly.

Figure 4 shows D_r of all the PEGs plotted as a function of casein concentration in casein suspensions at 20 °C. As the casein concentration increased, D_r decreased. Moreover, for a given casein concentration, the reduction in D_r was more pronounced for larger PEGs than smaller ones. It therefore appeared from these findings that the diffusion was sensitive to protein concentration and PEG size.

Effects of Gelation. Stejskal−Tanner plots are given for all the PEGs at a concentration of 16.44 g/100 g in casein gels (Figure 3). As already observed for the suspensions, all the curves showed linear regression except for 634 000 g/mol PEG in gels. For the latter, data were fitted with eq 2, which takes into account the polydispersity of the PEG.

Self-diffusion coefficients of 634 000 g/mol PEG were measured in a casein gel (16 g/100 g) with the PGSTE sequence for Δ values of 20, 100, 200, and 400 ms. The

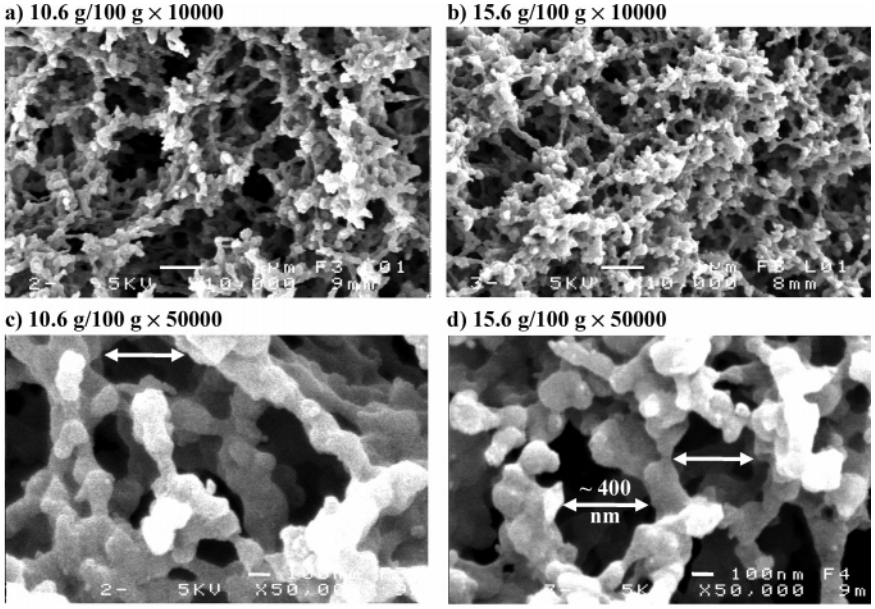

Figure 7. SEM images of rennet-induced casein gels at two casein concentrations and two magnifications: 10.6 g/100 g (a, c) 15.6 g/100 g (b, d).

Stejskal−Tanner plots are given in Figure 5. The self-diffusion coefficients at each Δ value were similar, indicating that no restricted diffusions were present and that the gel appeared homogeneous on the diffusion length scale of 2 μm. In other words, any inhomogeneities for instance in PEG concentration must have correlation lengths less than a few micrometers.

Figure 6 shows the PEG self-diffusion coefficient in suspensions divided by the PEG self-diffusion coefficient in gels, $D_{PEG}^{sol}/D_{PEG}^{gel}$, plotted as a function of the casein concentration for each PEG molecular masses.

Diffusion was sensitive to protein concentration and to PEG size, in both suspensions and gels. The $D_{PEG}^{sol}/D_{PEG}^{gel}$ ratio was close to one for the two smallest PEGs (1080 and 8500 g/mol) and confirmed the absence of influence of gelation on PEG diffusion. For the two largest PEGs (82 250 and 634 000 g/mol) $D_{PEG}^{sol}/D_{PEG}^{gel}$ was lower than one and decreased when the casein concentration increased. For the two largest PEGs the diffusion is faster in the gels than in the suspensions. This figure shows clearly that the effect of gelation on PEG diffusion was more pronounced at high protein concentrations and for the largest PEG. The diffusion of the 634 000 g/mol PEG in casein suspensions at high concentrations was the most affected by this change in structure.

SEM images of rennet-induced casein gels were made with two different casein concentrations and are presented in Figure 7 at different magnifications. The gels formed a homogeneous structure on a scale of 2 μm consistent with the linearity of the Stejskal−Tanner plot and with the constant values of D with the diffusion time Δ. The caseins formed a coarse and particulate network. The particles making up the strands are spherical with a thickness around 150 nm. The structure of the three-dimensional network consisted of multiple strands with chain junctions appearing as clusters of micelles and leaving large spaces in which serum can diffuse. The same organization was observed for all the concentrations. Spaces of ∼400 nm were observed on the high-magnification images. Therefore, the decrease of the PEGs diffusion coefficient as a function of the casein concentration could be interpreted as an effect of an increase of the volume fraction without any change of the gel structure.

Discussions

In Casein Solutions. Casein proteins exist in a colloidal particle known as the casein micelle. The micelles are fairly porous, the hydration value given in the literature[34−36] is about 4.5 g of H_2O/g of protein, and they have a diameter of ∼50−500 nm with a mean of 150 nm.[37]

The casein micelle structure has still not been determined, and numerous models have been proposed.[38−40] Among these models, the "open structure" model[41] and the "casein submicelle model"[42,43] are the most accepted.

In the "submicelle model" the micelle is constituted of subunits (∼10−20 nm in diameter) named submicelles. The submicelles are considered to be held together by nanocrystals of calcium phosphate and by hydrophobic and hydrogen bonds and are covered by a hydrophilic coat, which is at least partly composed of the polar moieties of κ-casein. The hydrophilic caseinomacropeptide of κ-casein exists as flexible hair located on the surface of the micelle.

The "open structure" model involves a more or less spherical, highly hydrated, and fairly open particle. Polypeptide chains in the core are partly cross-linked by nanometer sized clusters of calcium phosphate. The internal structure gives rise to an external region of lower segment density known as the hairy layer, which confers steric and/or charge stability on native casein particles.

McMahon et al.[44] have shown that the processes used during sample preparation for electron microscopy result in artifacts in micrograph casein micelles and give the micelle a submicellar appearance. They found that the submicelles are less densely packed than assumed and in micrographs the constituent proteins of the submicelles appear as individual proteins.

The high porosity of the micelle was recently illustrated from field-emission scanning electron microscopy (FESEM) images.[45] From the micrographs the surface of the micelle appeared to be formed from

cylindrical and tubular structures between 10 and 20 nm in diameter, protruding from the bulk of the micelle. These micrographs suggested that the surface of the casein micelle was more complex than a simple hard sphere covered by relatively short hairs. A number of "pores" were detected on some of the images, suggesting that the interior of the micelle might be readily accessible from its exterior.[45] A number of observations have demonstrated the permeability of the micelle: (i) The refrigeration of milk is known to induce reversible release of β-casein from the micelle to the serum phase. The ability of β-casein to diffuse outside the micelle is explained by the decrease in hydrophobic interactions under cooling.[46,47] (ii) The porous structure is also supported by the action of proteases such as transglutaminase. This large enzyme (45 000 g/mol) induces intramicellar cross-linking because of the ability to diffuse into the micelle.[48−51] (iii) Lastly, NMR studies have reported that the casein micelle has an open structure with a considerable amount of side-chain flexibility.[52−55]

Therefore, in agreement with the casein micelle structure model and with the high porosity of the casein particle, the PEG diffusion can be decomposed into two diffusion pathways: one around the micelle particle and one through the micelle particle. The linear attenuation of the NMR signal observed for all the concentrations regardless of PEG size demonstrated that the PEG molecules inside and outside the micelles were in fast diffusion exchange.

This is confirmed by the fact that the diffusion of the 1080 g/mol PEG at protein concentration of 15.5 g/100 g ($D_{PEG} = 1.21 \times 10^{-10}$ m^2 s^{-1} and $\Delta = 10$ ms) corresponds to a diffusion distance of 1.55 μm larger than the casein micelle diameter (~300 nm).

Moreover, the obstruction effect induced by an impenetrable spherical particle is known and depends only on the volume fraction of the obstructing particle:

$$D_r = \frac{1}{1+\frac{\phi}{2}} \tag{4}$$

with

$$\Phi = \frac{m^{cas}\nu^{cas} + m^{cas}H^{cas}\nu^{water}}{m^{cas}\nu^{cas} + m^{water}\nu^{water}} \tag{5}$$

The specific volume of casein micelles ν^{cas} is equal to 0.75 cm^3 g^{-1}, and H^{cas} is the hydration of casein micelle in g of H_2O/g. The voluminosity V^{cas} of casein micelles is equal to

$$V^{cas} = \nu^{cas} + H^{cas}\nu^{water} \tag{6}$$

According to this diffusion model, a D_r of 0.75 is expected at a concentration of 16.22 g/100 g ($\phi = 0.64$). This value is large compared to the experimental findings and demonstrates that the casein micelle could not be described as impenetrable particle. Moreover, this model did not allow to take into account the PEG size dependency.

To take into account two diffusion pathways, a general expression has been proposed by Jönsson et al.[56] and successfully used to explain the water self-diffusion coefficient in casein suspension and gels.[57,58] This model supposed was based on upon three main assumptions: (1) steric hindrance is the cause of the reduction of solute diffusion, and hydrodynamic interactions are negligible in the network studied; (2) the steric hindrance is caused by the static network (immobile micelles), not by the interaction with diffusing species; (3) the structure of the network is decomposed into a set of cylindrical cells, and the contribution from each cell to the diffusion coefficient is determined by the distribution of spaces in the network.

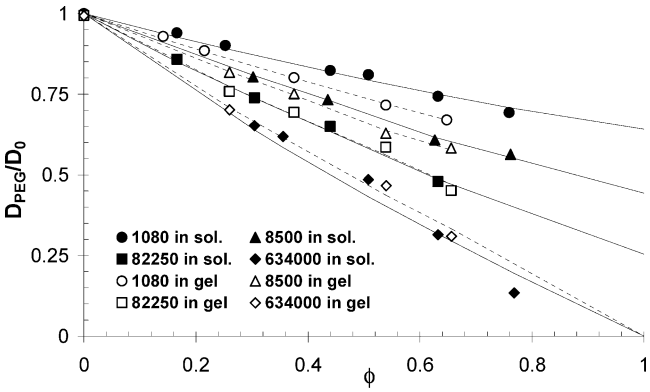

Figure 8. PEG self-diffusion coefficients vs casein volume fraction in solutions and gels. The solid and dashed lines are the fittings with the eq 7 of the cell model with $H^{cas} = 4.5$ g/g for solutions and $H^{cas} = 3.77$ g/g for gels.

In this model the hindrance due to the network is considered to depend not only on the size of the diffusant and the network concentration but also on the properties of the network, i.e., the thickness and stiffness.

According to Jönsson et al.,[56] when the size of the diffusive particle is small compared to the size of the obstructing particle, the observed self-diffusion is given by

$$D_{PEG} = D_2 \frac{1}{1-\left(1-\frac{C_1}{C_2}\right)\phi} \frac{1-\beta\phi}{1+\frac{\beta\phi}{2}} \tag{7}$$

with

$$\beta = \frac{D_2C_2 - D_1C_1}{D_2C_2 + 0.5D_1C_1} \tag{8}$$

where C_2 is the PEG concentration in aqueous phase varying as a function of casein concentrations given by

$$C_2 = \frac{C^{PEG}_{initial}}{m^{water} - m^{cas}} = \frac{0.1}{100 - \frac{C^{cas}\times 100}{C^{cas}+100}} \text{ g of PEG/ g of water} \tag{9}$$

D_2 is the PEGs self-diffusion coefficients in bulk water ($= D_0$), D_1 is the PEGs self-diffusion coefficients inside the micelles, and C_1 is the PEG concentrations in casein micelle defined by

$$C_1 = \frac{H^{cas}C_2}{1+H^{cas}} \text{ g of PEG/g of water} \tag{10}$$

The fitting of the data with the eq 7 requires knowing either D_1 or C_1 (which is function of H^{cas}). If H^{cas} is fixed, the PEG self-diffusion coefficient inside the micelle (D_1) become the only unknown parameter. Its value for each

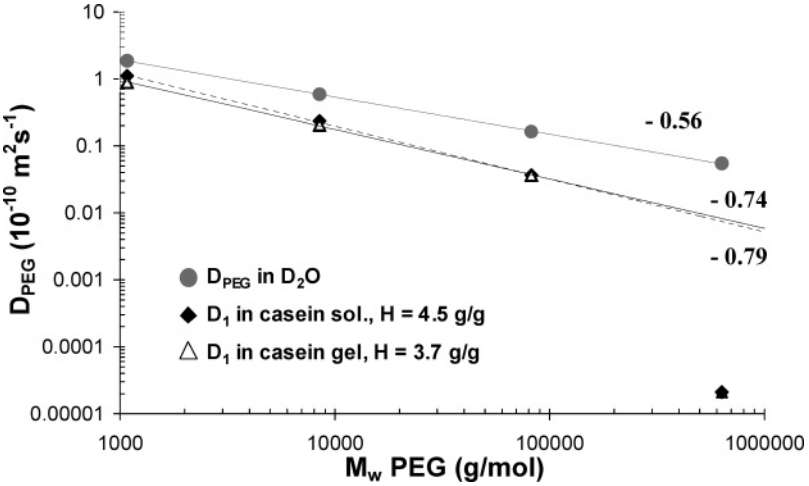

Figure 9. Power law representation of PEG self-diffusion coefficients in D_2O, inside the micelles (D_1): in solutions and in gels. The dashed and solid lines are the power law regression without the 634 000 g/mol PEG for D_1.

PEG could be obtained from the fitting of eq 7 to the experimental data. C_1 could be computed from values of H^{cas} taken from the literature. A hydration H^{cas} = 4.5 g of H_2O/g for all the casein concentration and all the PEGs permit to obtain a good fit to the experimental data whatever the PEG size (Figure 8) for $D_1 = 1.11 \times 10^{-10}$, 2.36×10^{-11}, 3.64×10^{-12} $m^2\ s^{-1}$, and 2.09×10^{-15} $m^2\ s^{-1}$ with 1080, 8500, 82 250, and 634 000 g/mol PEG, respectively. Using these values, a power law dependency of D_1 as a function of the PEG molecular mass was obtained and could be described by following equation:

$$D_{PEG} = AM_w^{-\alpha} \quad (11)$$

with A a preexponential factor and α a characteristic exponent. This relation is often proposed to describe the self-diffusion of polymer chains and α varied from 0.55 for diluted systems[59] to 2.5 for concentrated systems.[60] The results are presented in Figure 9. For PEGs of sizes up to 82250 g mol^{-1}, a good fit with eq 11 was obtained, and α was equal to 0.75. This value is close to α in D_2O (α = 0.55) and demonstrated a small effect of the internal casein micelle structure on the PEG diffusion. On the other hand, for 634 000 g mol^{-1} PEG size, the fit from the eq 11 was not possible, which suggested that for this molecular mass the PEG diffusion was strongly reduced by the internal structure of the casein micelle.

Gelled State. When casein gels are prepared through the addition of rennet enzyme, the stability of the dispersion of the casein particles was lost. Hairy layers of hydrophilic κ-casein at the surface of the casein micelles which account for (predominantly) steric stabilization were cut by rennet.[61−65] As a result, the rennet-altered micelles coagulate in the presence of Ca^{2+} (colloidal calcium phosphate[66]) at temperatures greater than 18 °C, eventually leading to the formation of the space-spanning structure.

Several aggregation steps have to be taken into account in the aggregation mechanism. In a comprehensive review, Mellema et al.[67] proposed casein micellar rearrangement to occur on four structural levels. The first is the rearrangement of subparticles. Here, fusion of primary particles can occur, resulting in particle deformation and contraction. The second level is interparticle rearrangement and involves changes in the mutual positions of the particles. This can be interpreted as particles rolling over each other. The third level comprises changes of the sizes of clusters, gel pores, or strands. Together with particle fusion, this process can lead to tensile stresses in strands nearby, stretching strands and possibly making them thinner.[68]

Following the interpretation of the findings in casein suspension, the coagulation effect can be explained by two mechanisms. First, a decrease of the casein particle voluminosity and of the effective size of the obstructing element induced by the cutting of the hairy layers. This effect would lead to the formation of a space-spanning structure in the network, and an increase in PEG diffusion would be expected.

Second, the fused particles can be accompanied by a reduction in strand porosity by shrinkage. This effect would lead to an increase in the obstruction effect for PEG molecules diffusing through the strands and thus a decrease in the diffusion coefficient.

In agreement with our findings, this mechanism seemed less likely than the first since an increase in diffusion was observed for the two largest PEGs after rennet coagulation. The absence of significant effect of coagulation for the smallest PEGs (1080 and 8500 g/mol) may be attributed to lower sensitivity to a change in voluminosity as observed in suspension because of their smaller size.

After renneting, several authors had measured a reduction of the casein micelle diameter between 7 and 15 nm.[39,69,70] With a casein mean diameter of 250 nm and a hydration of 4.5 g/g (V^{cas} = 5.25 cm^3/g) a decrease of 7.3 nm in diameter after renneting induce a casein micelle hydration around 3.77 g/g (V^{cas} = 4.52 cm^3/g). Equation 7 of the cell model applied to the experimental data in gels with H^{cas} = 3.77 g of H_2O/g is shown in Figure 8. A good fit was obtained for all PEG sizes for $D_1 = 8.90 \times 10^{-11}$, 2.0×10^{-11}, 3.64×10^{-12}, and 2.09×10^{-15} $m^2\ s^{-1}$ for 1080, 8500, 82 250, and 634 000 g/mol PEG, respectively. This demonstrates that a decrease of the casein micelle voluminosity after renneting is sufficient to explain the PEGs diffusion in casein gels. The power law dependency of D_1 in gels is shown in Figure 9. No significant variations of D_1 values in casein gels were observed compared to D_1 in casein solutions; by considering the three smallest PEGs, the value of D_1 is the same in the two systems (0.78 against 0.73). As already mentioned for casein in solution, the diffusion coefficient D_1 for the 634 000 g/mol PEG was not

correctly described by eq 11. This deviation could be explained by the large size of this PEG (~39 nm) too close to the size of the casein particle.

Conclusions

It has been clearly shown that the PEG diffusion in casein suspensions and gels is affected by protein concentration and PEG size and is sensitive to gelation.

In agreement with the high porosity of the casein particle, the obstruction can be decomposed in two diffusion pathways: one around the micelle particle and one through the micelle particle: the greater the PEG size, the greater the confinement induced by the internal casein structure. Variations in diffusion coefficient related to casein concentrations could be explained by the balance between the obstruction effects induced by micelle particles and internal micelle porosity.

The results could be well explained by the cell model of Jönsson et al. by fixing the casein micelle voluminosity in casein solutions to 5.25 cm^3/g and deducing the internal PEG self-diffusion coefficient D_1. In casein gels, a decrease of the voluminosity to 4.52 g of H_2O/g due to the hydrolysis of the κ-casein has given new values of D_1. No significant variations between D_1 in solutions and gels were found for the three smallest PEG, and a power law dependency was found. An important decrease of D_1 for the 634 000 g/mol PEG was attributed to the large size of the PEG compared to the casein micelle involving screening interactions.

Acknowledgment. The authors thank the Regional Council of Brittany and Lund University for financial support. Roxane Colsenet thanks the Marie Curie Training Site (Contract HPMT-CT-2000-00150), and Olle Soderman thanks the Swedish Research Council (VR). We are grateful to Mr. Armel Guillermo for helpful discussions about NMR experiments and Mr. Joseph Le Lannic for assistance with the SEM experiments.

References and Notes

(1) Callaghan, P. T.; Komlosh, M. E.; Nyden, M. *J. Magn. Reson.* **1998**, *133*, 177−182.
(2) Atha, D. H.; Ingham, K. C. *J. Biol. Chem.* **1981**, 12108−12117.
(3) Bhat, R.; Timasheff, S. N. *Protein Sci.* **1992**, *1*, 1133−1143.
(4) Hancock, T. J.; Hsu, J. T. *Biotechnol. Bioeng.* **1996**, *51*, 410−421.
(5) Hermans, J. *J. Chim. Phys.* **1982**, *77*, 2193−2203.
(6) Knoll, D.; Hermans, J. *J. Biol. Chem.* **1983**, *258*, 5710−5715.
(7) Johansson, L.; Shantze, U.; Lofroth, J. E. *Macromolecules* **1991**, *24*, 6019−6023.
(8) Brown, W.; Stilbs, P. *Polymer* **1982**, *24*, 188−192.
(9) Masaro, L.; Zhu, X. X.; Macdonald, P. M. *Macromolecules* **1998**, *31*, 3880−3885.
(10) Masaro, L.; Zhu, X. X.; MacDonald, P. M. *J. Polym. Sci., Part B: Polym. Phys.* **1999**, *37*, 2396−2403.
(11) Walderhaug, H.; Kjoniksen, A. L.; Nystrom, B. *J. Phys. Chem. B* **1997**, *101*, 8892−8897.
(12) Walderhaug, H.; Nystrom, B. *Colloids Surf., A* **1999**, *149*, 379−387.
(13) Jo, B. W.; Hess, M.; Zahres, M. *Mater. Res. Innov.* **2003**, *7*, 178−182.
(14) Petit, J. M.; Zhu, X. X.; Macdonald, P. M. *Macromolecules* **1996**, *29*, 70−76.
(15) Griffiths, P. C.; Stilbs, P.; Yu, G. E.; Booth, C. *J. Phys. Chem.* **1995**, *99*, 16752−16756.
(16) Hakansson, B.; Nyden, M.; Söderman, O. *Colloid Polym. Sci.* **2000**, *278*, 399−405.
(17) Favre, E.; Leonard, M.; Laurent, A.; Dellacherie, E. *Colloids Surf. A: Physicochem. Eng. Asp.* **2001**, *194*, 197−206.
(18) Masaro, L.; Ousalem, M.; Baille, W. E.; Lessard, D.; Zhu, X. X. *Macromolecules* **1999**, *32*, 4375−4382.
(19) Matsukawa, S.; Ando, I. *Macromolecules* **1996**, *29*, 7136−7140.
(20) Matsukawa, S.; Ando, I. *Macromolecules* **1997**, *30*, 8310−8313.
(21) Skirda, V. D.; Aslanyan, I. Y.; Philippova, O. E.; Karybiants, N. S.; Khokhlov, A. R. *Macromol. Chem. Phys*. **1999**, *200*, 2152−2159.
(22) Kwak, S.; Lafleur, M. *Colloids Surf., A* **2003**, *221*, 231−242.
(23) Trampel, R.; Schiller, J.; Naji, L.; Stallmach, F.; Kärger, J.; Arnold, K. *Biophys. Chem.* **2002**, *97*, 251−260.
(24) Newling, B. *J. Phys. Chem. B* **2003**, *107*, 12391−12397.
(25) Naji, L.; Schiller, J.; Kaufmann, J.; Stallmach, F.; Kärger, J.; Arnold, K. *Biophys. Chem.* **2003**, *104*, 131−140.
(26) Johansson, L.; Elvingson, C.; Lofroth, J. E. *Macromolecules* **1991**, *24*, 4, 6024−6029.
(27) Masaro, L.; Zhu, X. X. *Langmuir* **1999**, *15*, 8356−8360.
(28) Matsukawa, S.; Ando, I. *Macromolecules* **1999**, *32*, 1865−1871.
(29) Colsenet, R.; Soderman, O.; Mariette, F. *Magn. Reson. Imaging* **2005**, *23*, 347−348 (Sp. Iss).
(30) Alper, J. S.; Gelb, R. I. *J. Phys. Chem.* **1990**, *94*, 4747−4751.
(31) Koppel, D. E. *J. Chem. Phys.* **1972**, *57*, 4814−4820.
(32) Callaghan, P. T.; Pinder, D. N. *Macromolecules* **1983**, *16*, 968−973.
(33) Metais, A.; Cambert, M.; Riaublanc, A.; Mariette, F. *J. Agric. Food. Chem.* **2004**, *52*, 3988−3995.
(34) Stothart, P. H.; Cebula, D. J. *J. Mol. Biol.* **1982**, *160*, 391−395.
(35) Kumosinski, T. F.; Pessen, H.; Farrell, H. M., Jr.; Brumberger, H. *Arch. Biochem. Biophys.* **1988**, *266*, 548−561.
(36) Farrer, D.; Lips, A. *Int. Dairy J.* **1999**, *9*, 281−286.
(37) Fox, P. F.; McSweeney, P. L. H. In *Dairy Chemistry and Biochemistry*; Chapman and Hall: London, 1999.
(38) Rollema, H. S. In *Advanced Dairy Chemistry Proteins*; Fox, P. F., Ed.; Elsevier Applied Science: London, 1992; pp 111−140.
(39) Walstra, P. *J. Dairy Sci.* **1979**, *46*, 317−323.
(40) Cayot, P.; Lorient, D. *Structures et technofonctions des protéines du lait*; Lavoisier: Paris, 1998.
(41) Holt, C.; Horne, D. S. *Neth. Milk Dairy J.* **1996**, *50*, 85−111.
(42) Schmidt, D. G. *Neth. Milk Dairy J.* **1980**, *34*, 42−64.
(43) Walstra, P. *Int. Dairy J.* **1999**, *9*, 189−192.
(44) McMahon, D. J.; McManus, W. R. *J. Dairy Sci.* **1998**, *81*, 2985−2993.
(45) Dalgleish, D. G.; Spagnuolo, P.; Douglass Goff, H. *Int. Dairy J.* **2004**, *14*, 1025−1031.
(46) Creamer, K.; Berry, G. P.; Mills, O. E. *New Zeal. J. Dairy Sci.* **1997**, *12*, 58.
(47) Dalgeish, D. G.; Law, J. R. *J. Dairy Res.* **1989**, *56*, 727−735.
(48) De Kruif, C. G.; Tuinier, R.; Holt, C.; Timmins, P. A.; Rollema, H. S. *Langmuir* **2002**, *18*, 4885−4891.
(49) O'Connell, J. E.; De Kruif, C. G. *Colloids Surf., A* **2003**, *216*, 75−81.
(50) Schorsch, C.; Carrie, H.; Norton, I. T. *Int. Dairy J.* **2000**, *10*, 529−539.
(51) Schorsch, C.; Carrie, H.; Clark, A. H.; Norton, I. T. *Int. Dairy J.* **2000**, *10*, 519−528.
(52) Griffin, M. C.; Roberts, G. C. *Biochem. J.* **1985**, *228*, 273−276.
(53) Rollema, H. S.; Brinkhuis, A.; Vreeman, H. J. *Neth. Milk Dairy J.* **1988**, *42*, 233−248.
(54) Rollema, H. S.; Brinkhuis, J. A. *J. Dairy Sci.* **1989**, *56*, 417−425.
(55) Kakalis, L. T.; Kumosinski, T. F.; Farrell, H. M., Jr. *Biophys. Chem.* **1990**, *38*, 87−98.
(56) Jönsson, B.; Wennerstrom, H.; Nilsson, P. G.; Linse, P. *Colloid Polym. Sci.* **1986**, *264*, 77−88.
(57) Mariette, F.; Topgaard, D.; Jonsson, B.; Soderman, O. *J. Agric. Food Chem.* **2002**, *50*, 4295−4302.
(58) Colsenet, R.; Cambert, M.; Mariette, F. *J. Agric. Food Chem.*, in press.
(59) De Gennes, P. G. *Nature (London)* **1979**, *282*, 367−370.
(60) Tao, H.; Lodge, T. P.; von Meerwall, E. D. *Macromolecules* **2000**, *33*, 1747−1758.
(61) De Kruif, C. G. *Int. Dairy J.* **1999**, *9*, 183−188.
(62) Horne, D. S. *Int. Dairy J.* **1998**, *8*, 171−177.
(63) Zoon, P.; Van Vliet, T.; Walstra, P. *Neth. Milk Dairy J.* **1988**, *42*, 295−312.

(64) Walstra, P. *J. Dairy Sci.* **1990**, *73*, 1968−1979.
(65) Dalgleish, D. G. In *Cheese: Chemistry, Physics and Microbiology*; Fox, P. F., Ed.; Chapman & Hall: London, 1993; Vol. 1, pp 69−100.
(66) Zhang, Z. P.; Aoki, T. *Int. Dairy J.* **1996**, *6*, 769−780.
(67) Mellema, M.; Walstra, P.; Van Opheusden, J. H. J.; Van Vliet, T. *Adv. Colloid Interface Sci.* **2002**, *98*, 25−50.
(68) Gastaldi, E.; Lagaude, A.; Delafuente, B. T. *J. Food Sci* **1996**, *61*, 59−65.
(69) Walstra, P.; Bloomfield, V. A.; Wei, G. J.; Jenness, R. *Biochim. Biophys. Acta* **1981**, *669*, 258.
(70) Alexander, M.; Dalgleish, D. G. *Colloids Surf., B* **2004**, *38*, 83−90.

MA051294H